Acta Crystallographica Section D

Volume 70 (2014)

Supporting information for article:

Diamonds in the rough: a strong case for the inclusion of weak-intensity X-ray diffraction data

Jimin Wang and Richard A. Wing

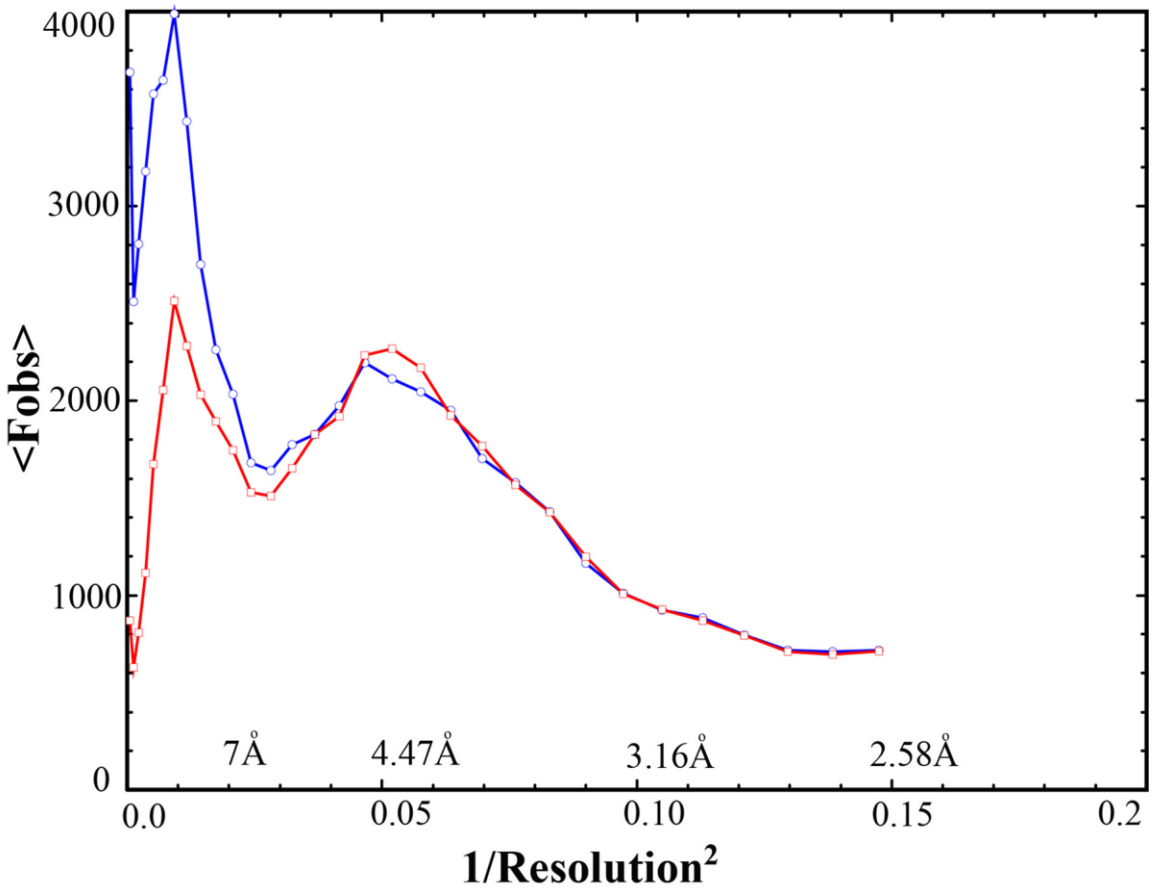

Figure S1 Amplitude distribution as a function of resolution for reflections with (h+k+l=2n) in blue and for reflections with (h+k+l=2n+1) in red for the pseudo-tNCS vector of (1/2, 1/2, 1/2).

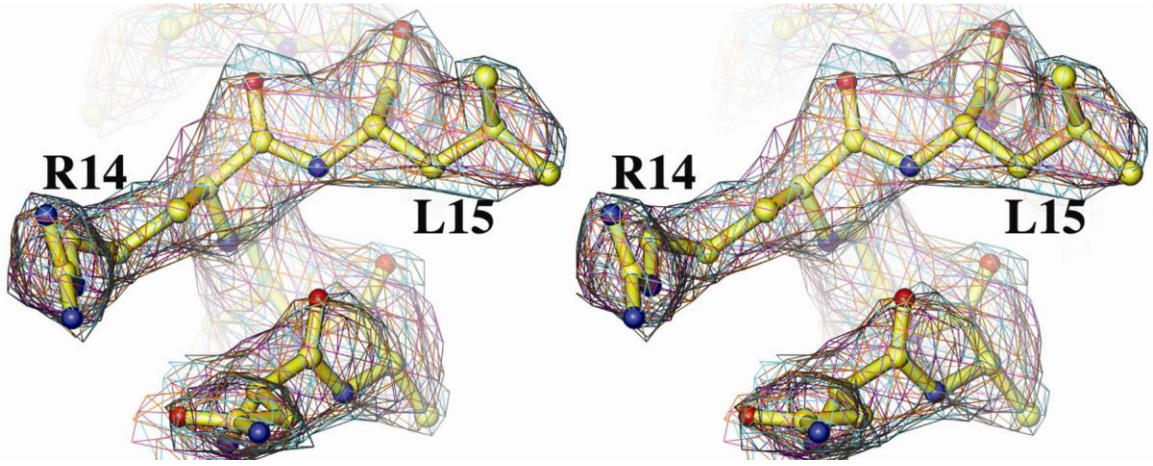

Figure S2 Stereodiagram of the experimental maps at 2.5-Å (cyan), 2.8-Å (golden), and 3.1-Å resolution (magenta), respectively, contoured at 1 σ.

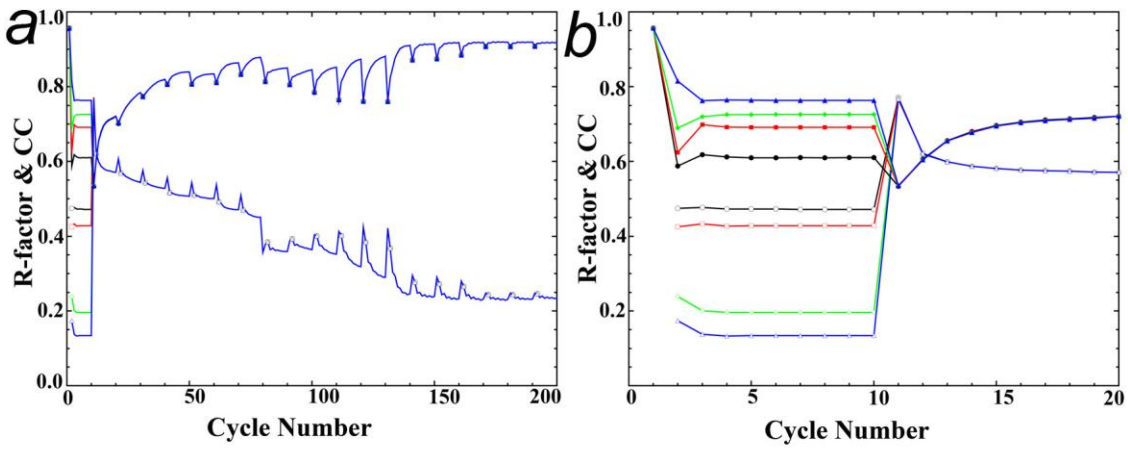

Figure S3 NCS averaging statistics with gradually reduced amount of experimental phases in initial map calculation. R-factors and electron density correlation coefficients are shown in open and filled objects. The resolution of initial experimental phases was reduced to 20-Å (black), 30-Å (red), and 40 (green)-Å resolution; and finally, the only 2 reflections (blue) were included as initial map calculations. Panel (b) is a close-up view of panel (a). After 10 cycles, all curves are precisely superimposed on top of each other.

S1. Purification, crystallization, data collection, and do novo NCS averaging

Endogenous YfbU was obtained as a contaminant during purification of rat nucleoporins from *E. coli* strain BL21-CodonPlus™(DE3)-RIL in three steps. First, frozen cell pellets were resuspended in Buffer 1 (10 mM Tris pH 8.0, 250 mM NaCl, 5 mM β-mercaptoethanol, 5 mM imidazole) supplemented with 5 mM phenylmethylsulfonyl fluoride (PMSF) and lysed by passage through a cell disruptor three times. Second, clarified lysate was incubated with HisSelect® nickel beads for 30 min at 4°C and eluted with a modified Buffer 1 that contained 150 mM imidazole (as Buffer R). Third, after overnight dialysis of the elute into Buffer A (10 mM Tris pH 8.0, 100 mM NaCl, 0.5 mM EDTA, 1 mM DTT), sample was further purified over a Hi-Trap Q column equilibrated in Buffer 2 using a gradient from 0 to 500 mM NaCl. Fractions containing rat nucleoporins of interest were retained and mixed with an additional nucleoporin. The mix of both sets of nucleoporins was unfolded by adding Buffer U1 (10 mM Tris pH 8.0, 0.5 mM EDTA, 1 mM DTT, 6 M Urea) to the relevant fractions in a ratio of 2 volumes of Buffer U1 to 1 volume of Buffer A plus salt. A refolding reaction was setup by diluting the mix with Buffer U2 (10 mM Tris pH 8.0, 1 mM DTT, 0.5 mM EDTA) slowly over 2 days using a peristaltic pump. The refolding reaction was further dialyzed into fresh Buffer U2 a second time overnight.

Finally, the refolded complex of nucleoporins was purified using size-exclusion chromatography containing all individual components with no trace of other proteins apparent via SDS-PAGE analysis. Finally, the complex was concentrated to a final concentration of 10.5 mg / mL in Buffer U2 and flash frozen in liquid nitrogen.

Crystals were obtained in 1.8 M ammonium phosphate monobasic and either 100 mM Tris pH 8.5 or 100 mM MES pH 5.5 using standard vapor diffusion at 16°C. Drops were prepared by adding 1 μL of the refolded complex at 10.5 mg / μL to 1 μL of the well solution. The crystals reached full size after one month, were equilibrated stepwise into 1.6 M ammonium phosphate monobasic, either 100 mM Tris pH 8.5 or 100 mM pH 5.5 consistent with their crystallization condition, and 20% glycerol for cryoprotection and frozen in liquid nitrogen. For initial experimental phasing, crystals were soaked with Tri-Sodium Phosphotungstate (Jena Biosciences) at a concentration of 500 μM for between 1 hour and 8 days in the above described cryoprotection solution. Data were collected at beamlines 24ID-C and 24ID-E of the Advanced Photon Source at Argonne National Laboratories as well as beamlines X-25 and X-29 of National Synchrotron Light Source at Brookhaven National Laboratory.

In retrospect, given the known NCS matrices and particle masks derived from previous runs of NCS averaging, we succeeded the NCS averaging with only 2 low-resolution phased reflections (Fig. S3). These averaging procedures rapidly converged to a state with the statistics that were indistinguishable to the averaging procedure starting with 10-Å resolution experimental phases. In this averaging, we did not impose the positive density constraints due to missing all low-resolution reflections between 230 and 54 Å near the beam-stop in the X-ray diffraction data. With different signs of the initially assigned value in uniform maps, resulting electron densities differed by negation, and phases differed by π due to the Babinet ambiguity. We further carried out the NCS averaging using an initial spherical shell mask with diameters derived from the atomic structure to represent the YfbU particle. Resulting maps had many recognizable features of α-helices, suggesting that we could obtain an accurate mask for the particle through mask refinement using mask-less NCS averaging. Prior to mask refinement, four sets of phases could result from the NCS averaging using the symmetric shell masks with equal probability: right- or left-handed structure or its negated densities due to handedness and Babinet ambiguities, i.e., αP, -αP, αP+π –αP+π, respectively, where αP represents the phases of the right-handed protein structure. Once the certain unique features of electron densities are recognizable in the NCS averaging using partially refined masks, we can readily convert all phase solutions to those of the right-handed structure with positive densities through a simple arithmetic transformation of resulting phases.